

Transverse Momentum of ψ and Dimuon Production in Pb+Pb Collisions

Sean Gavin^{a,b} and Ramona Vogt^{c*}

^aPhysics Department, Brookhaven National Laboratory, Upton, New York, 11973

^bPhysics Department, Columbia University, New York, New York, 10027

^cInstitute for Nuclear Theory, University of Washington, Seattle, Washington, 98195

(July 13, 2021)

CERN collaboration NA50 has measured charmonium and Drell–Yan dimuon production in Pb+Pb collisions. Parton scattering broadens the transverse momentum, p_T , distributions for these processes. We predict that $\langle p_T^2 \rangle$ will flatten in Pb+Pb collisions as a function of the neutral transverse energy of hadrons, E_T , in contrast to the almost–linear rise seen in $S+U \rightarrow \psi + X$. If seen, such a flattening will support hadronic explanations of charmonium suppression.

preprint: CU-TP-791, DOE/ER/40561-292-INT96-21-01

The NA50 collaboration at the SPS has reported a suppression of ψ production in Pb+Pb collisions relative to Drell–Yan dimuon production as the neutral transverse energy of hadrons, E_T , is increased [1]. They further presented a striking ‘threshold effect’ by comparing the data to S+U results as a function of a calculated quantity, the mean path length of the ψ through nuclear matter, L . The NA50 comparison is shown in fig. 1; the open symbols are from ref. [1]. In this note, we demonstrate that the relation between L and the measured E_T is model dependent. However, we point out that measurements of the centrality dependence of the transverse momenta of Drell–Yan dimuons essentially provide an experimental determination of L . We argue that such a determination can provide vital evidence for – or against – the threshold behavior, which has been linked to the onset of quark–gluon plasma formation in the Pb system [1,2].

To see how the path length affects the ‘threshold’ interpretation of the NA50 comparison, we replot the Pb+Pb data using $L(E_T)$ calculated with eq. (3) and the realistic nuclear densities [3] that were employed in [4]. We see that the appearance of the data is very sensitive to small changes in the definition of L . With the realistic L , one no longer gets the impression that the Pb+Pb data “departs from a universal curve.” This departure has been cited as evidence [1] that Pb collisions cross a threshold and form quark–gluon plasma.

In ref. [4], we observed that the Pb+Pb data are in good accord with predictions of charmonium suppression using a hadronic comover model [5,6]. While these predictions are supported by cascade calculations [7], the plasma explanation cannot be excluded. We attributed the behavior of fig. 1 to a geometric saturation that occurs in the symmetric Pb+Pb system, but not in asymmetric S+U collisions; we discuss this below. We see in fig. 1 that the saturation phenomena, though softened, does not vanish with our calculated $L(E_T)$. Saturation – the flattening of $L(E_T)$ – indeed occurs in our scenario, but only as a consequence of geometry.

Important information on the suppression mechanism can be extracted from the nuclear dependence of the ψ ’s

transverse momentum, p_T . The hadronic suppression in ref. [4,5] does not modify the transverse momentum dependence of ψ production appreciably [8]. To account for the nuclear modification measured in pA and S+U collisions, initial–state parton scattering was introduced [9,10]. Bodwin, Brodsky and Lepage and, independently, Michael and Wilk had predicted that initial– and final–state parton scattering can modify the momentum distributions of hard interactions in nuclear collisions [11]. Evidence for such scattering has been seen in a variety of hadron–nucleus experiments [12–14].

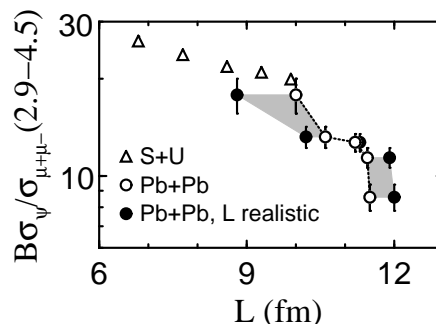


FIG. 1. Comparison of NA50 Pb+Pb (open circles) and NA38 S+U (open triangles) data as in [1]. Data replotted with a realistic $L(E_T)$ from eqs. (3,7) appear different. The gray area represents the uncertainty in this presentation of the data due to $L(E_T)$.

Initial–state scattering [11] is elastic at the parton level and broadens the p_T distributions of charmonium and Drell–Yan production without affecting the p_T –integrated yields [9,10]. Partons essentially undergo a random walk in momentum space, so that $\langle p_T^2 \rangle$ grows linearly with L . Initial–state scattering provides the only nuclear effect proposed so far that can modify the p_T distribution in the Drell–Yan process in a manner consistent with data [12,13]. While other effects such as comover scattering can alter the p_T distribution in charmonium

production, we find in practice that the contributions to $\langle p_T^2 \rangle$ are small if the comovers are assumed to be hadrons (see [9] and the discussion below). Measurements of $\langle p_T^2 \rangle$ – particularly for dimuons – can therefore provide *experimental* information on L .

If $\langle p_T^2 \rangle$ increases with L as in hadronic models of charmium suppression incorporating initial-state scattering, then the geometric saturation in Pb collisions implies a flattening of $\langle p_T^2 \rangle$. In contrast, if the threshold interpretation [1] is correct and the Pb results are the consequence of a new contribution to ψ suppression from quark–gluon plasma, then one would not expect $\langle p_T^2 \rangle$ to flatten with E_T . If observed, a flattening would lend strong support to the comover explanation. Alternatively, if no flattening is observed, then our hadronic model would be excluded. Plasma suppression is currently thought to be strongly p_T dependent [15], although models with a weaker dependence (and without thresholds) have been presented [16].

Plasma issues aside, measurements of $\langle p_T^2 \rangle$ can help remove the model dependence of fig. 1 [1]. Gerschel and Hüfner [17] pointed out that a plot similar to fig. 1 but containing only measured quantities can be constructed by replacing L with the measured $\langle p_T^2 \rangle$ of the ψ . Measurements of the $\langle p_T^2 \rangle$ of the Drell–Yan process, though more difficult, can provide a clearer determination of L .

In this paper we update the description of initial-state scattering from ref. [9] using more recent information from FNAL pA experiment E772 [13]. We then derive an expression for the path length L , and study its behavior as a function of E_T for S+U and Pb+Pb collisions. Finally, we combine these results to predict the behavior of $\langle p_T^2 \rangle$ for Pb+Pb collisions.

In a hadron–nucleus collision, a parton from the projectile can suffer soft quasielastic interactions as it crosses the nuclear target on its way to the hard process. We follow [9] and assume that in each nucleon–nucleon, NN , subcollision there is a fixed probability ϕ that the parton is affected. In a hadron–nucleus collision, the $\langle p_T^2 \rangle$ of the dimuon or ψ is then increased by:

$$\Delta p_T^2 \equiv \langle p_T^2 \rangle - \langle p_T^2 \rangle_{NN} = \lambda^2 (\bar{n}_A - 1), \quad (1)$$

where \bar{n}_A is the number of NN subcollisions that the projectile suffers in the target and $\lambda^2 \propto \phi$ determines the increment to the projectile parton’s p_T^2 from each subcollision. We subtract ‘1’ to eliminate the hard subcollision that produces the ψ or dimuon from \bar{n}_A and introduce $\langle p_T^2 \rangle_{NN}$ to account for the A -independent contribution from that subcollision. The impact parameter averaged total number of subcollisions grows with the target radius $R_A \approx 1.2 A^{1/3}$ as $\bar{n}_A \approx 3\sigma_{NN}\rho_0 R_A/2 \approx 0.77 A^{1/3}$, where ρ_0 is the average nuclear density and $\sigma_{NN} \approx 32$ mb is the inelastic NN cross section.

In ref. [9], transverse momentum distributions measured in hadron–nucleus collisions by CERN NA10 and NA3 [12] were used to fix $\langle p_T^2 \rangle_{NN}$ and λ for Drell–Yan and ψ production. In fig. 2, we compare Δp_T^2 from

eq. (1) with more recent data from a larger number of nuclear targets presented by FNAL E772 [13]. The random walk behavior, $\Delta p_T^2 \propto A^{1/3}$, is evident. This approximation agrees roughly with calculations using realistic nuclear densities as in ref. [18]. In this work we take $\lambda_{\mu^+\mu^-} \approx 0.18 \pm 0.01$ GeV and $\lambda_\psi \approx 0.36 \pm 0.03$ GeV for Drell–Yan and ψ production. These values are chosen to agree with E772 and NA3 data, respectively. They are compatible with the idea that initial-state scattering is a soft process. We will use NA38 S+U data to obtain $\langle p_T^2 \rangle_{NN}$ below.

Observe that our Drell–Yan value is somewhat smaller than the 0.24 ± 0.05 GeV value used in ref. [9]. This spread perhaps reflects the systematic uncertainty (not included in the fit uncertainty) in comparing experiments with different kinematic coverages. E772 did not report Δp_T^2 for ψ , but did give results for Υ production, a process that likely has similar initial-state interactions. A fit to that data implies $\lambda_\Upsilon \approx 0.46$ GeV, which is larger than our $\lambda_\psi = 0.36$ GeV. The values that we have taken above are the smaller of the choices.

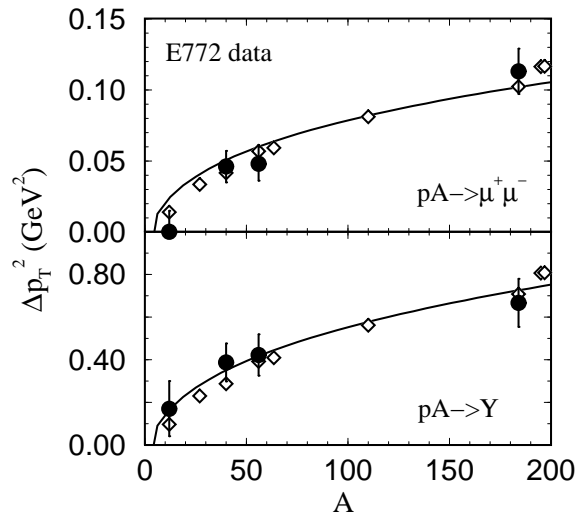


FIG. 2. Calculated Δp_T^2 from eq. (1) for $\bar{n}_A \approx 0.77 A^{1/3}$ compared to FNAL E772 data on the Drell–Yan process and Υ production [13]. Diamonds are calculated using (4) and JVV nuclear densities from [3].

We remark on the interpretation of the parameters in eq. (1). In ref. [9], the value of the ratio $(\lambda_\psi/\lambda_{\mu^+\mu^-})^2 \sim 2.3$ had been attributed to the 9/4 enhancement of the cross section for gluon–gluon relative to quark–gluon forward scattering. The initial-state partons are predominantly gluons for ψ production and quarks and antiquarks for the Drell–Yan process, because the primary production mechanisms for ψ and dilepton production are gluon fusion and quark–antiquark annihilation, respectively. In contrast, the parameters that we now use imply a ratio $(\lambda_\psi/\lambda_{\mu^+\mu^-})^2 \sim 3.9$ that is $\sim 70\%$ larger than the earlier estimate, while E772 values alone suggest $(\lambda_\Upsilon/\lambda_{\mu^+\mu^-})^2 \sim 6.8$. The perturbative estimate

$(\lambda_\psi/\lambda_{\mu^+\mu^-})^2 \sim 9/4$ [10,19] may not be correct in detail, since λ^2 involves small momentum transfers. Nevertheless, this disagreement is quite large.

If taken literally, a larger ratio can suggest that the ψ also undergoes final-state elastic scattering as it escapes the nucleus. During its escape, the nascent ψ is not a fully formed hadron but, rather, a $c\bar{c}$ pair. This pair can be in a color octet state and, therefore, can scatter essentially as a gluon does. Fortunately, this final-state octet scattering also follows eq. (1), so that we can describe this effect in conjunction with initial-state gluon scattering by replacing λ^2 with $2\lambda^2$. Together with the 9/4 color factor, this factor can roughly account for the ratio of λ^2 in ψ and $\mu^+\mu^-$. However, this observation is speculative. Therefore, we will not include the factor of two explicitly, but merely stress the possibility that the empirical λ for charmonium production receives contributions from both initial- and final-state octet scattering.

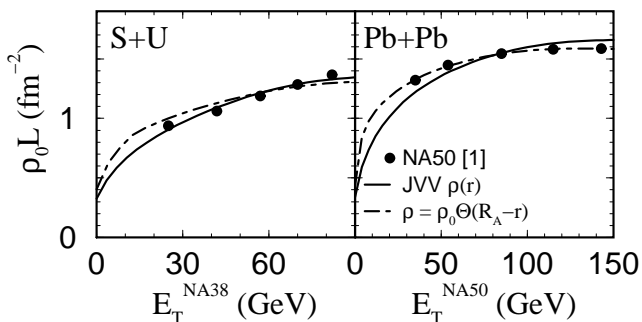


FIG. 3. NA50 $L(E_T)$ [1] (points) compared to calculations for the JVV nuclear densities [3] (solid) and for a sharp-surface approximation (dot-dashed).

In a nucleus-nucleus collision, both projectile and target partons scatter. We then write

$$\Delta p_T^2 \equiv \langle p_T^2 \rangle - \langle p_T^2 \rangle_{NN} = \lambda^2(\bar{n}_A + \bar{n}_B - 2). \quad (2)$$

The NA50 path length is

$$L \equiv (\bar{n}_A + \bar{n}_B)/2\sigma_{NN}\rho_0 \equiv \bar{n}/2\sigma_{NN}\rho_0. \quad (3)$$

The relation between \bar{n} and the impact parameter \vec{b} depends on the collision geometry. A nucleon at a transverse position \vec{s} in the projectile can undergo

$$n_A = \sigma_{NN} \int_{-\infty}^z dz' \rho_A(\vec{s}, z'), \quad (4)$$

subcollisions prior to its hard interaction at longitudinal position z , where ρ_A is the projectile density. The expression for the number of subcollisions suffered by a nucleon at a transverse position $\vec{b} - \vec{s}$ in the target is similar. Since the hard process occurs with a probability density $\propto \rho_A(\vec{s}, z)\rho_B(\vec{b} - \vec{s}, z')$, the average number of subcollisions for a given b is

$$\bar{n}(b) = \frac{\sigma_{NN}}{T_{AB}} \int d^2s T_A(s)T_B(|\vec{b} - \vec{s}|)[T_A(s) + T_B(|\vec{b} - \vec{s}|)], \quad (5)$$

where $T_{A,B} = \int_{-\infty}^{\infty} dz' \rho_{A,B}$ are the nuclear thickness functions and $T_{AB} = \int d^2s T_A(s)T_B(|\vec{b} - \vec{s}|)$. An alternative derivation of eq. (5) in the spirit of ref. [17] is given in ref. [19].

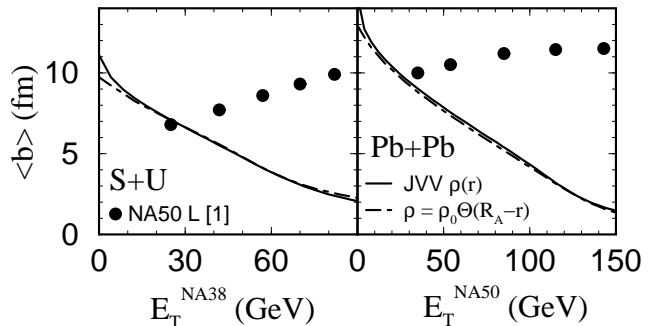


FIG. 4. Average impact parameter as a function of E_T for realistic nuclear densities (solid) and for a sharp-surface approximation (dot-dashed). NA50 $L(E_T)$ [1] (points) are included for comparison.

To obtain the E_T dependence of \bar{n} – and therefore $L(E_T)$ – we fold eq. (5) with the probability $P(E_T, b)$ that a collision at impact parameter b produces transverse energy E_T . This probability is related to the minimum-bias distribution by

$$\sigma_{\min}(E_T) = \int d^2b P(E_T, b). \quad (6)$$

The distribution $P(E_T, b)$ depends both on the collision geometry and the calorimeter type. We use the phenomenological $P(E_T, b)$ relevant to the NA50 Pb+Pb collisions from ref. [4]; this parametrization schematically incorporates fluctuations at fixed b due to both collision dynamics and detector effects. The average number of collisions for a given E_T is then

$$\bar{n}(E_T) = \sigma_{NN} \langle T_A(s) + T_B(|\vec{b} - \vec{s}|) \rangle, \quad (7)$$

where we now average over the weighted product of the densities,

$$\langle \dots \rangle \equiv N^{-1} \int d^2b d^2s P(E_T, b)T_A(s)T_B(|\vec{b} - \vec{s}|)(\dots), \quad (8)$$

with $N = \int d^2b P(E_T, b)T_{AB}$ (c.f. eq. (5)).

We now compute $L(E_T)$ using eqs. (3,7) and (8). In fig. 3 we compare the NA50 $L(E_T)$ [1] to the path length calculated using two assumptions for the nuclear density profile. Following ref. [4], we use the realistic three-parameter Woods-Saxon densities from deJager, deVries

and deVries (JVV) [3]. We compared this to a sharp-surface approximation $\rho = \rho_0 \Theta(R_A - r)$. NA38 [20] obtained L for S+U from ψ p_T data using a phenomenological procedure that is essentially equivalent to eqs. (2, 3), while NA50 calculated L assuming the sharp-surface approximation [21]. Consequently, we see that the NA50 Pb+Pb values agree with our sharp-surface results, while the NA38 S+U values are nearer to the realistic-density computations. [The calculation of L is not described in ref. [1], so the agreement of our sharp-surface $L(E_T)$ with the NA50 Pb result is an important check.] Note that to compare to the NA50 calculations, we plot $\rho_0 L$ rather than L because the authors of ref. [1] use a value $\rho_0 = 0.138 \text{ fm}^{-3}$.

We see that $L(E_T)$ saturates in Pb+Pb collisions, as observed in ref. [4]. To see why saturation occurs in this system but not in S+U, we compare the NA50 $L(E_T)$ [1] to the average impact parameter $\langle b \rangle(E_T)$ in fig. 4. We use the JVV densities to compute $\langle b \rangle = \langle b T_{AB} \rangle / \langle T_{AB} \rangle$. [Note that NA50 reports similar values of $\langle b \rangle(E_T)$ [1].] For all but the highest E_T bin addressed by the S+U measurement, we see that $\langle b \rangle$ is near $\sim R_S = 3.6 \text{ fm}$ or larger. In this range, increasing b dramatically reduces the collision volume and, consequently, L . In contrast, in Pb+Pb collisions $\langle b \rangle < R_{\text{Pb}} = 6.6 \text{ fm}$ for $E_T > 50 \text{ GeV}$, so that L does not vary appreciably.

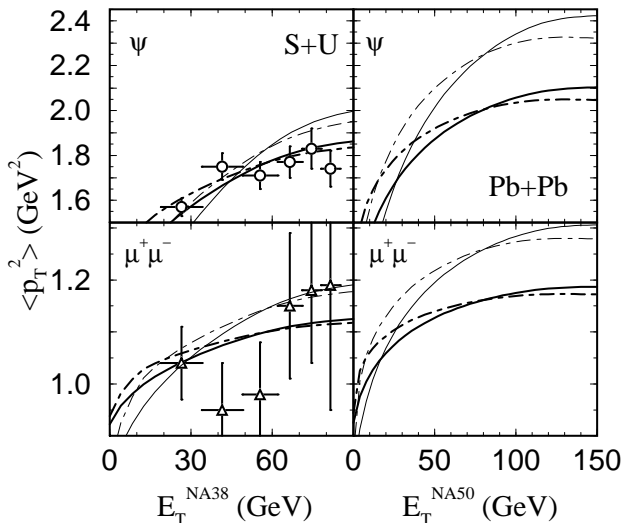


FIG. 5. The calculated E_T dependence of $\langle p_T^2 \rangle$ for ψ (upper plots) and Drell-Yan dimuons (lower plots) in S+U and Pb+Pb collisions. The calculations are performed for realistic nuclear densities (solid) and for the sharp-surface approximation (dot-dashed). NA38 S+U data is from [22]. The thick curves are computed for our preferred values, $\lambda_\psi = 0.36 \text{ GeV}$ and $\lambda_{\mu^+\mu^-} = 0.18 \text{ GeV}$, while the thin curves are for $\lambda_\psi = 0.46 \text{ GeV}$ and $\lambda_{\mu^+\mu^-} = 0.24 \text{ GeV}$.

We now use eqs. (2, 7) to compute Δp_T^2 for both the Drell-Yan process and ψ production as functions of E_T in S+U and Pb+Pb collisions. Our results are shown

in fig. 5. Parton-scattering calculations agree with S+U data from ref. [22]. Observe that to compare to the NA38 S+U data, we fit the data to extract $\langle p_T^2 \rangle_{NN} \approx 0.92$ and 1.07 GeV^2 for Drell-Yan pairs and ψ respectively. Note that the ψ value is somewhat smaller than the $1.23 \pm 0.05 \text{ GeV}^2$ reported by NA3 and used in ref. [9]; this is likely another indication of systematic uncertainties.

To illustrate the spread in the Pb predictions implied by the uncertainty in the parameters, we compute the thin curves in Fig. 5 by taking $\lambda_\psi \approx \lambda_\Upsilon = 0.46 \text{ GeV}$ from E772 and $\lambda_{\mu^+\mu^-} = 0.24 \text{ GeV}$ from [9]. With these values, we obtain the best agreement with the NA38 data for $\langle p_T^2 \rangle_{NN} \approx 0.81$ and 0.6 GeV^2 for dimuons and ψ , respectively. The modified ψ results are inconsistent with the S+U data. The modified dimuon results are consistent, although the agreement is somewhat better for our preferred value, $\lambda_{\mu^+\mu^-} = 0.18 \text{ GeV}$.

The thick curves for Pb+Pb collisions in fig. 5 represent our predictions. We expect $\langle p_T^2 \rangle$ to increase by 12.3% for ψ as E_T increases from 50 to 150 GeV. This represents a flattening of $\langle p_T^2 \rangle(E_T)$ in comparison to the S+U $\rightarrow \psi + X$ data, which show an 18.5% increase as E_T varies from 30 to 90 GeV. The flattening would be even more dramatic if the NA50 sharp-surface approximation (the dot-dashed curve in fig. 5) were true — $\langle p_T^2 \rangle$ would increase by only 6.8% for ψ and 2.7% for dimuons. While such small differences seem difficult to resolve, agreement with S+U $\rightarrow \psi + X$ data is better for the realistic L than for the sharp-surface result. Furthermore, NA38 [20,21] used this ψ data to obtain L values in agreement with our realistic calculation and quite distinct from our sharp-surface result. However, we stress that the most direct extraction of L comes not from ψ but from Drell-Yan dimuons. To check that the NA50 plot [1] is correct, *i.e.* to decide between the open circles and filled circles in fig. 1, Drell-Yan data in Pb+Pb would have to establish a 2.7% increase in $\langle p_T^2 \rangle$. This requires dimuon data far more precise than that for S+U collisions.

One can ask if elastic scattering of the ψ by comovers can affect its transverse momentum distribution. As mentioned earlier, comover absorption has only a marginal effect on the p_T distribution; its influence on $\langle p_T^2 \rangle$ is negligible [8,9]. However, elastic comover scattering can in principle allow the ψ to be pushed transversely, adding to its p_T . The argument [8,15] that elastic scattering with hadronic comovers is negligible follows from photoproduction data. The measured elastic ψN cross section is $\sim 0.079 \pm 0.012 \text{ mb}$ [23], accounting for only $\sim 2 - 4\%$ of the total cross section. The corresponding mean-free path for elastic scattering with hadronic comovers greatly exceeds the estimated size of the system, so that the ψ will not follow the comover flow. The general relation between scattering and flow is discussed in ref. [24]. One possible hole in this argument is that $\psi\pi$ scattering in the comover gas is likely below the $D\bar{D}$ dissociation threshold and, therefore, predominantly elastic. Another possible hole is that comovers need not be

hadrons.

The consistency of the NA38 S+U $\rightarrow \psi + X$ data in fig. 5 with (2) supports our neglect of elastic comover scattering. Nevertheless, if Pb+Pb experiments find a $\langle p_T^2 \rangle$ for ψ that is larger than our prediction *and* if other hadronic species show evidence of substantial transverse flow, it will be necessary to introduce elastic scattering into the comover scenario. This is best done in the context of cascade models.

In summary, we have predicted the nuclear enhancement of $\langle p_T^2 \rangle$ in Pb+Pb collisions as a function of E_T for charmonia and Drell–Yan dimuons, assuming that this enhancement is caused by quasielastic parton scattering. Such scattering has been included [9,10,15] in hadronic models of ψ suppression, where it is essential for describing the p_T dependence of pA , O+U and S+U data. We stress that the Drell–Yan process is unaffected by final–state comover or plasma interactions, so that a comparison of both ψ and $\mu^+\mu^-$ calculations to data can disentangle model uncertainties in $L(E_T)$ from new physics. In particular, the L extracted from dimuon measurements can confirm or disprove the threshold behavior claimed by NA50.

The parameters in the model were revised from an earlier work [9] to describe the latest E772 $pA \rightarrow \mu^+\mu^- + X$ data. Our revision implies a ratio $(\lambda_\psi/\lambda_{\mu^+\mu^-})^2 \sim 3.9$, larger than that extracted earlier [9], perhaps indicating that additional final–state scattering of the octet $c\bar{c}$ occurs in the charmonium case. More precise $pA \rightarrow \psi + X$ measurements are needed to explore this very interesting possibility.

We are grateful to Claudie Gerschel for discussing details of the NA38/50 data and to Mark Strikman for his careful reading of the manuscript. We also thank Miklos Gyulassy, Raffaele Mattiello and Bill Zajc for discussions. This work was supported in part by the U. S. Department of Energy under Contract Numbers DE-FG02-93ER40764 and DE-AC03-76SS0098.

- D. Kahana, S. H. Kahana and Y. Pang, Proc. RHIC Summer Study '96, BNL, Upton, NY, D. Kahana, S. H. Kahana and Y. Pang, in press (1996); L. Gerland *et al.*, in progress.
- [8] J. Ftacnik, P. Lichard, J. Pisut, Phys. Lett. 207B (1988) 194; S. Gavin, M. Gyulassy and A. Jackson, Phys. Lett. 207B (1988) 257; R. Vogt, M. Prakash, P. Koch and T. H. Hansson, Phys. Lett. 207B (1988) 263; J. Ftacnik, P. Lichard, N. Pisutova and J. Pisut, Z. Phys. C42, (1989) 132.
- [9] S. Gavin and M. Gyulassy, Phys. Lett. 214B (1988) 241; S. Gavin, AIP Conf. Proc. 243 (1992) 879.
- [10] J. Hüfner, Y. Kurihara, and H. J. Pirner, Phys. Lett. 215B (1988) 218; J.-P. Blaizot and J.-Y. Ollitrault, Phys. Lett. 217B (1989) 392.
- [11] G. T. Bodwin *et al.*, Phys. Rev. Lett. 47 (1981) 1799; C. Michael and G. Wilk, Z. Phys. C10 (1981) 169.
- [12] P. Bordalo *et al.* (NA10), Phys. Lett. B193 (1987) 373; J. Badier *et al.* (NA3), Z. Phys. C20 (1983) 101.
- [13] D. M. Alde *et al.* (E772), Phys. Rev. Lett. 66 (1991) 133, 2285.
- [14] M. D. Corcoran and A. S. Carroll, AIP Conf. Proc. 338 (1995) 375.
- [15] See, e.g. J.-P. Blaizot and J.-Y. Ollitrault in 'Quark-Gluon Plasma', R.C. Hwa ed. (World Scientific, 1991) p 631.
- [16] T. Matsui, Ann. Phys. (NY) 196 (1989) 182.
- [17] C. Gerschel and J. Hüfner, Z. Phys. C56 (1992) 171.
- [18] L. L. Frankfurt and M. I. Strikman, Nucl. Phys. B250 (1985) 143.
- [19] S. Gavin, Proc. RHIC Summer Study '96, BNL, Upton, NY, D. Kahana, S. H. Kahana and Y. Pang eds., in press, hep-ph/9609470 (1996).
- [20] A. Borhani, NA38, Ph. D. Thesis, l'Ecole Polytechnique (1996).
- [21] C. Gerschel, NA50, private communications.
- [22] C. Baglin *et al.* (NA38) Phys. Lett. 262B (1991) 362.
- [23] J. J. Aubert *et al.*, Nucl. Phys. B213 (1983) 1.
- [24] M. Prakash, M. Prakash, R. Venugopalan and G. Welke, Phys. Rep. 227 (1993) 321.
- [25] M. C. Abreu *et al.*, Nucl. Phys. A566 (1994) 77c.

* Permanent addresses: Lawrence Berkeley National Laboratory, Berkeley, CA, 94720 and University of California, Davis, CA, 95616.

- [1] M. Gonin *et al.* (NA50), Proc. Quark Matter '96, Heidelberg, Germany, P. Braun-Munzinger *et al.*, eds. (1996).
- [2] J.-P. Blaizot and J.-Y. Ollitrault, Phys. Rev. Lett. 77 (1996) 1703; D. Kharzeev, hep-ph/9609260 (1996).
- [3] C. W. deJager, H. deVries and C. deVries, Atomic Data and Nuclear Data Tables 14 (1974) 485.
- [4] S. Gavin and R. Vogt, hep-ph/9606490 (1996).
- [5] S. Gavin and R. Vogt, Nucl. Phys. B345 (1990) 104.
- [6] S. Gavin, H. Satz, R. L. Thews, and R. Vogt, Z. Phys. C61 (1994) 351; S. Gavin, Nucl. Phys. A566 (1994) 383c.
- [7] W. Cassing and C. M. Ko, nucl-th/9609025 (1996);